Discriminant-based bistability analysis of a TMG-induced lac operon model supported with boundedness and local stability results

Neslihan AVCU[1,*]**, Güleser KALAYCI DEMİR**[1]**, Ferhan PEKERGİN**[2]**,**
Hakan ALYÜRÜK[3]**, Levent CAVAS**[4]**, Cüneyt GÜZELİŞ**[5]

[1]Department of Electrical-Electronics Engineering, Faculty of Engineering, Dokuz Eylül University, İzmir, Turkey
[2]Laboratory of Informatics of Paris-North, Paris 13 University, French National Center
for Scientific Research (CNRS), Paris, France
[3]Graduate School of Natural and Applied Sciences, Dokuz Eylül University, İzmir, Turkey
[4]Department of Chemistry, Faculty of Science, Dokuz Eylül University, İzmir, Turkey
[5]Department of Electrical-Electronics Engineering, Faculty of Engineering Yaşar University,
İzmir, Turkey

Abstract: This paper presents the results of a theoretical and numerical study on the analysis of bistable behavior of the most studied gene regulatory network, the lac operon, in terms of the model parameters. The boundedness of the state variables for the considered model are demonstrated, the parameter values providing the existence of the multiple equilibria and thus the bistable behavior are determined, and a local stability analysis of the equilibria is performed. The parameter region yielding the existence of multiple equilibria is determined in an algebraic way based on discriminants. The model given in the state equation form is defined by the ordinary differential equations with the rational right-hand sides constituted within Hill and Michaelis–Menten approaches based on enzyme kinetics. The presented method can also be used in the parametric studies of other gene regulatory and metabolic networks given by state equations with rational right hand sides.

Key words: Lac operon, bistability, discriminant, gene regulatory networks, TMG

1. Introduction

The lactose operon, abbreviated as lac operon, of *Escherichia coli* (E. coli), which is responsible for controlling the lactose metabolism, operates as a bistable hysteretic switch under glucose starvation [1]. This bistable behavior of the lac operon has been investigated by many researchers in the literature [2–5]. These studies on the lactose regulation system of *E. coli* do not only provide a description of the gene regulation in glucose starvation in the existence of lactose, but also they are helpful to understand a variety of gene regulatory mechanisms in other organisms.

Although many efforts have been attempted to analyze the bistability behavior of the lac operon, the entire bistability ranges of the parameters related to the enzyme kinetics and also the reasons for the variations in the appearance of bistability across different inducers, e.g., lactose, methyl β-D-thiogalactopyranoside (TMG), or isopropyl-β-D-thiogalactopyranoside (IPTG), across the population of *E. coli* and across different experimental settings are not completely determined yet [5–7]. The main aim of this paper is to derive the entire ranges of the

---

*Correspondence: neslihan.avcu@deu.edu.tr

model parameters ensuring the bistability for a TMG-induced lac operon. A TMG-induced lac operon model is considered in the paper since this nonmetabolized lactose analog is usually preferred in most experimental studies. The parametric conditions on the bistability of the considered TMG-induced lac operon model are obtained in the presented work based on the discriminant of the (polynomial) equilibrium equation. The identified bistability ranges confirm and further extend the results available in the literature [2–5,8]. It is also shown that the condition $K > 9$ on the parameter K defining the basal activity in the considered model, which is reported in the literature [3,8] as the bistability condition for a variety of lac operon models, is one of the necessary condition only as opposed to the common consideration. For the sake of establishing a thorough bistability analysis, the equilibrium analysis performed in the presented work by applying a discriminant-based method to the polynomial equilibrium equation is supported by a complementary study on the boundedness of the state variables together with the local stability of the equilibrium points.

In the literature, the behavior of the lac operon is generally modeled by using ordinary differential equations (ODEs) derived from enzyme kinetics [3,4,7,8]. The delay-time ordinary differential equation systems and stochastic models are also presented in the literature [4]. In the deterministic models, the reaction rates are expressed as the time derivatives of molecule concentrations. The resulting systems of ODEs defining the lac operon become nonlinear, or more precisely rational functions of molecule concentrations when Michaelis–Menten and/or Hill approaches are used to model enzyme kinetics [3,4,6–9]. Although they are nonlinear, ODE models are quite efficient for numerical and also theoretical analyses. The stochastic models that are introduced for low molecule concentrations are derived usually either by choosing reaction rates as random variables in terms of the numbers of molecules or by introducing a noise term to the ODE models [9]. The stochastic models suffer from high computational costs; however, they can be preferred especially for modeling the interactions involving small numbers of molecules and the spontaneous transitions between the induced and uninduced states.

The TMG-induced lac operon model considered in this paper is derived from enzyme kinetics as a three-dimensional nonlinear ODE system in the state equation form whose right-hand sides are rational functions of the TMG, messenger ribonucleic acid (mRNA), and permease concentrations. The rational right-hand side state equations yielding polynomial equilibrium equations provide the possibility of determining the parameter values, ensuring the existence of triple equilibria required for the bistable behavior by using the discriminant of the polynomial equilibrium equation.

The developed discriminant-based method provides a parametric equilibrium analysis of the rational right-hand sided ODE models without having any information about the values of model parameters, thus constituting a solution to the problem of analysis of the lac operon and also the other general gene regulatory network models under parameter uncertainties. The determined bistability ranges for the lac operon model parameters are also helpful for understanding the variations in the appearance of the bistable behavior of the biological lac operon, which is observed to show differences from one species to another and even from one experiment to another.

Section 2 of this paper presents the considered mathematical model for the TMG-induced lac operon together with biological explanations for the modeled molecular interactions. The analysis results on the boundedness of the trajectories and the local stability of the equilibrium points are given in Section 3. The bistability ranges of the model parameters are determined in Section 4 by using the proposed discriminant-based bistability analysis method. Section 4 also presents the graphical representations of the bistability region to evaluate and compare with the results available in the literature.

2. A model of the lac operon

The lac operon is the gene region of *E. coli* that synthesizes the enzymes to metabolize lactose as a carbon source under glucose starvation [1]. It consists of three structural genes, namely *LacZ*, *LacY*, and *LacA*. *LacZ*, *LacY*, and *LacA* produce permease, β-galactosidase, and transacetylase enzyme, respectively. The first one, permease, provides the transportation of external lactose into the cell through the cell membrane. The second one, β-galactosidase, is responsible for the cleavage of the internal lactose to the allolactose, while the third one, transacetylase, is included in the sugar metabolism and the acetylation reaction [3]. The operation mode of the lac operon is controlled by another gene, the regulatory gene *LacI*. In the presence of glucose, the repressor protein LacI binds to the promoter part of the lac operon to prevent the expression of gene products, and so *E. coli* does not use the lactose as a carbon source.

The basal activity of the cell always causes small amounts of permease and β-galactosidase enzymes inside the cell [1–6]. The transfer of the lactose from the medium into the cell and the conversion of the internal lactose to allolactose are provided by the small amounts of these two enzymes in the absence of glucose and the existence of lactose in the extracellular medium. The allolactose binds to the LacI repressor protein, thus causing a conformational change in the repressor and inhibiting the repressor by dissociating it from the promoter region. The RNA polymerase enzyme then starts transcription of mRNA by binding the free promoter site of the lac operon to synthesize the three structural genes. By this process, the gene products of the lac operon, i.e. permease, β-galactosidase, and transacetylase, increase rapidly from the basal levels to much higher levels.

The increase in the permease and β-galactosidase concentrations also elevates the concentrations of the internal lactose and allolactose. The mutual amplification of the allolactose and mRNA concentrations implies a positive feedback in the lactose metabolism [3,4]. In general, the positive feedback is known to be a source of unstable dynamics in a system. In a living cell, the mRNA concentration is bounded below and above, respectively, by the basal and saturation activities, which provide two stable equilibria: one at a low concentration corresponding to the uninduced state for the lac operon and the other at a high concentration corresponding to the induced state [3]. The coexistence of these induced and uninduced stable states, which has been observed in experimental studies, provides a bistable behavior for the lac operon [3,4,6–9].

Two different suppression mechanisms are present in the cell when glucose exists. The first one in path I is called catabolite repression, as given Figure 1. In catabolite repression mechanism, the presence of glucose yields decreasing cAMP concentrations in the cell. The decrease in cAMP concentration leads to a lack of binding cAMP to CRP, i.e. the cAMP receptor protein, to form CAP complex. Thus, mRNA transcription cannot be induced due to the lack of CAP complex. This means that the glucose leads the lac operon into the uninduced state. The other mechanism is path II, called inducer exclusion; the glucose inhibits the transport of the external lactose into the cell by interfering with the permease activity, leading to the exclusion of the inducer, i.e. lactose.

In experimental studies, it is generally preferred to use lactose analogs such as TMG and IPTG instead of natural inducer lactose. These artificial inducers are not metabolized and do not interact with β-galactosidase enzyme. Therefore, the β-galactosidase enzyme concentration becomes an irrelevant variable in the response of the lac operon to artificial inducers. However, similar to allolactose, the artificial inducers inhibit the LacI repressor, leading to the transcription of mRNA and consequently to the production of permease at higher concentrations. These features make the artificial inducers efficient for experimental studies on the bistable dynamics of the lac operon [3,4].
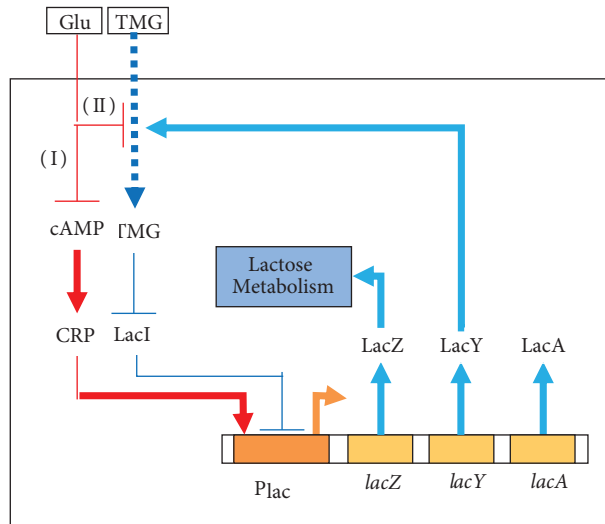
Figure 1. Lac operon gene regulatory network.

The presented study considers a simple yet sufficient ODE model in which an artificial inducer, TMG, is used. The mathematical model consists of three ODEs in the state equation form with the mRNA, permease, and TMG concentrations as state variables. The considered model includes: i) the catabolite repression and inducer exclusion of the extracellular glucose, ii) the transcription of mRNA by TMG, iii) the production of permease, iv) the transportation of TMG via permease, and v) the degradations of TMG, mRNA, and permease. It is assumed that there are no translational and transcriptional delays in the lac operon mechanism. As will be seen, this model is very suitable for analyzing the hysteretic bistable behavior of the lac operon.

The model in the paper is described by the following state model, which is composed of three first-order differential equations representing the reaction rates in terms of the mRNA, permease, and internal TMG concentrations:

$$\frac{dM}{dt} = \alpha_M f_{M,T}(T) f_{M,Ge}(Ge) - \gamma_M M, \tag{1}$$

$$\frac{dP}{dt} = \alpha_P M - \gamma_P P, \tag{2}$$

$$\frac{dT}{dt} = \alpha_T f_{T,Te}(Te) f_{T,Ge}(Ge) P - \gamma_T T, \tag{3}$$

where state variables M, P, and T stand for the mRNA, permease, and internal TMG concentrations, respectively. The inputs T_e and G_e stand respectively for external TMG and external glucose concentration. The parameters γ_i with $i \in \{M,P,T\}$ represent the loss constants for M, P, and T; γ_i is indeed the composition of the active degradation, $\bar{\gamma}_i$, and the dilution due to growth rate, μ_i. The parameters α_i with $i \in \{M,P,T\}$ denote the production constants of the gene products. $f_{M,T}(T)$ and $f_{M,Ge}(Ge)$ express the positive effect of the internal TMG and the negative effect of the external glucose on the synthesis of mRNA, respectively. Similarly, $f_{T,Te}(Te)$ and $f_{T,Ge}(Ge)$ express the positive effects of external TMG and negative effects of external glucose on the TMG uptake into the cell. Here, $f_{M,Ge}(Ge)$ and $f_{T,Ge}(Ge)$ are decreasing functions of external glucose; the former describes the catabolite repression while the latter describes the inducer exclusion.

In the model, the temporal change of the mRNA concentration is defined in Eq. (1) as the difference between the production depending on the internal TMG concentration under the catabolite repression effect of external glucose and the losses due to the active degradation and growth. Eq. (2) gives the change of the permease concentration in terms of the synthesized permease and the losses. Similarly, the change of the internal TMG concentration is expressed in Eq. (3), where the increase is due to the import of the external TMG under the reduction effect of inducer exclusion and the decrease is due to the degradation and dilution.

Assuming the production of mRNA under TMG as an allosteric interaction, similar to the allolactose case, $f_{M,T}(T)$ can be chosen as the following modified Hill function [10].

$$f_{M,T}(T) = \frac{1 + K_1 T^n}{K + K_1 T^n},\tag{4}$$

where n is the number of TMG molecules required to inactivate a repressor protein, K_1 is the equilibrium constant of TMG-repressor protein interaction, and $1/K$ is the basal level of mRNA transcription in $E.\ coli$. For the inhibition of repressor protein, at least two TMG molecules have to bind the repressor. n is taken as 2 in our analysis throughout the study [10].

The transport of T_e into the cell by the permease can be modeled via Michaelis–Menten kinetics as follows:

$$f_{T,T_e}(T_e) = \frac{T_e}{K_{T_e} + T_e},\tag{5}$$

where K_{T_e} is the Michaelis constant [4]. The monotonically decreasing functions of G_e for describing the catabolite repression and inducer exclusion are chosen as follows:

$$f_{M,G_e}(G_e) = \frac{K_{M,Ge,1} + G_e^m}{K_{M,Ge,2} + K_{M,Ge,3}G_e^{\,m}},\tag{6}$$

$$f_{T,G_e}(G_e) = 1 - \beta_{T,G_e}\frac{G_e}{K_{T,G_e} + G_e},\tag{7}$$

where $K_{M,Ge,1}$, $K_{M,Ge,2}$, $K_{M,Ge,3}$, and m are catabolite repression parameters and β_{T,G_e} and K_{T,G_e} are the inducer exclusion parameters [11].

3. Boundedness of the state variables, existence of multiple equilibria, and local stability analysis of the lac operon model

The bistable dynamics for a system can be defined by the existence of two (locally) asymptotically stable equilibria such that any trajectory of the system tends toward one of these equilibria depending on the initial condition if not starting at a possible unstable equilibrium. This implies the boundedness of the state variables of the system dynamics and also excludes other kinds of dynamics such as limit cycle and chaos.

This section describes that the considered model in Eqs. (1)–(3) has bounded dynamics and multiple equilibria, and it presents a local stability analysis of the equilibria of the model in Eqs. (1)–(3).

3.1. Boundedness of the state variables

The loss terms in Eqs. (1)–(3) are linear. Thus, considering the (nonlinear) production terms as inputs for first-order linear differential equations, one can obtain an analytical expression for each of the state variables of

the model in Eqs. (1)–(3):

$$M\left(t\right) = e^{-\gamma_M\left(t-t_0\right)}M\left(t_0\right) + \int_{t_0}^{t} e^{-\gamma_M\left(t-\tau\right)}\alpha_M f_{M,T}\left(T\left(\tau\right)\right)f_{M,G_e}\left(G_e\right)d\tau, \tag{8}$$

$$P\left(t\right) = e^{-\gamma_P\left(t-t_0\right)}P\left(t_0\right) + \int_{t_0}^{t} e^{-\gamma_P\left(t-\tau\right)}\alpha_P M\left(\tau\right)d\tau, \tag{9}$$

$$T\left(t\right) = e^{-\gamma_T\left(t-t_0\right)}T\left(t_0\right) + \int_{t_0}^{t} e^{-\gamma_T\left(t-\tau\right)}\alpha_T f_{T,T_e}\left(T_e\right)f_{T,G_e}\left(G_e\right)P\left(\tau\right)d\tau. \tag{10}$$

As expressed in Eqs. (4)–(6), the production function of the mRNA and the catabolite repression effect of the G_e are bounded above.

$$\left|f_{M,T}(T)\right| = \left|\frac{1 + K_1 T^2}{K + K_1 T^2}\right| < 1\, for\, K > 1 \tag{11}$$

$$\left|f_{M,G_e}\left(G_e\right)\right| = \left|\frac{K_{M,Ge,1} + G_e^m}{K_{M,Ge,2} + K_{M,Ge,3}G_e{}^m}\right| \leq \frac{K_{M,Ge,1}}{K_{M,Ge,2}} \tag{12}$$

Note that $K > 1$ is always true, as observed from experimental studies [3]. An upper bound for the mRNA concentration is then obtained as follows:

$$\left|M\left(t\right)\right| \leq e^{-\gamma_M\left(t-t_0\right)}M\left(t_0\right) + \frac{\alpha_M}{\gamma_M}\frac{K_{M,Ge,1}}{K_{M,Ge,2}}\left[1 - e^{-\gamma_M\left(t-\tau\right)}\right]. \tag{13}$$

The following upper bound for the permease concentration is found in a similar way.

$$\left|P\left(t\right)\right| \leq e^{-\gamma_P\left(t-t_0\right)}P\left(t_0\right) + \frac{\alpha_P}{\gamma_P}\left|M\left(t\right)\right|\left[1 - e^{-\gamma_P\left(t-\tau\right)}\right] \tag{14}$$

Considering the following bounds for $f_{T,Te}\left(Te\right)$ and $f_{T,Ge}\left(Ge\right)$

$$\left|f_{T,T_e}(T_e)\right| = \left|\frac{T_e}{K_{T_e} + T_e}\right| \leq 1 \tag{15}$$

$$\left|f_{T,G_e}\left(G_e\right)\right| = \left|1 - \beta_{T,G_e}\frac{G_e}{K_{T,G_e} + G_e}\right| \leq 1 \tag{16}$$

an upper bound for the internal TMG concentration is derived as:

$$\left|T\left(t\right)\right| \leq e^{-\gamma_T\left(t-t_0\right)}T\left(t_0\right) + \frac{\alpha_T}{\gamma_T}\left|P\left(t\right)\right|\left[1 - e^{-\gamma_T\left(t-\tau\right)}\right] \tag{17}$$

The expressions given in Eqs. (13), (14), and (17) show the boundedness of the state variables $M\left(t\right)$, $P(t)$, and $T(t)$. As can be seen from the limits of the upper bounds given in Eqs. (18), (19), and (20), the model in Eqs. (1)–(3) is indeed eventually uniformly bounded [12].

$$\exists t_M > 0 \ni \left|M\left(t\right)\right| \leq \frac{\alpha_M}{\gamma_M}\frac{K_{M,Ge,1}}{K_{M,Ge,2}}\forall t \geq t_M \tag{18}$$

$$\exists t_P > 0 \ni |P(t)| \le \frac{\alpha_P}{\gamma_P}\frac{\alpha_M}{\gamma_M}\frac{K_{M,Ge,1}}{K_{M,Ge,2}}\forall t \ge t_P \tag{19}$$

$$\exists t_T > 0 \ni |T(t)| \le \frac{\alpha_T}{\gamma_T}\frac{\alpha_P}{\gamma_P}\frac{\alpha_M}{\gamma_M}\frac{K_{M,Ge,1}}{K_{M,Ge,2}}\forall t \ge t_T \tag{20}$$

Since the functions in Eqs. (12), (15), and (16) are continuous functions of the lac operon inputs (i.e. external glucose and external TMG), so are the upper bounds of the states, and then the lac operon defined by Eqs. (1)–(3) is concluded to be bounded-input bounded-state (BIBS) stable [12].

3.2. Existence of multiple equilibria

In this subsection, it is shown that the considered model has either one or three equilibrium points depending on the model parameters. Setting the state variables M, P, and T constant and then eliminating the equilibrium concentrations M and P the equilibrium equation for T can be obtained as:

$$pf_{M,T}(T) - T = p\frac{1 + K_1 T^2}{K + K_1 T^2} - T = 0, \tag{21}$$

where

$$p = \frac{\alpha_T}{\gamma_T}\frac{\alpha_P}{\gamma_P}\frac{\alpha_M}{\gamma_M}f_{T,T_e}(T_e) f_{T,G_e}(G_e) f_{M,G_e}(G_e). \tag{22}$$

As illustrated in Figure 2, the production function $f_{M,T}(T)$ of mRNA starts at $1/K$ and tends asymptotically to 1 irrespective of the parameters K and K_1. $1/K > 0$ and the continuity of $f_{M,T}(T)$ together with the saturation characteristic imply that the graph of $pf_{M,T}(T)$ intersects the unity slope line corresponding to the second term T in Eq. (21). This proves the existence of at least one equilibrium point. Furthermore, $f_{M,T}(T)$ is a monotically increasing function, since its derivative,

$$\frac{d}{dT}f_{M,T}(T) = \frac{d}{dT}\left\{\frac{1 + K_1 T^2}{K + K_1 T^2}\right\} = \frac{2K_1 T(K - 1)}{(K + K_1 T^2)^2} \tag{23}$$

is positive for $K > 1$ that is always true. However, the derivative of $pf_{M,T}(T)$ is not monotonic and is less than 1 for sufficiently small and large T values and greater than 1 for intermediate T values. Depending on the value of the parameter p, the graphs of the first and second terms in Eq. (21) may have three intersection points as shown in Figure 1, which means there are three equilibria for the considered model.

The below graphical analysis provides an insight into the appearance of bistability, which requires the existence of three equilibria, two of them stable. However, determining the ranges of the parameters ensuring the existence of multiple equilibria requires a rigorous analysis. Considering the availability of well-established methods for the parametric studies of the roots of polynomial equations, it is convenient to rearrange the equilibrium equation (Eq. (21)) into the following polynomial form.

$$K_1 T^3 - pK_1 T^2 + KT - p = 0. \tag{24}$$

It is obvious that, irrespective of the values of the parameters, there is always a real root of Eq. (24), indicating the existence of at least one equilibrium point. The remaining two roots of Eq. (24) are either a complex conjugate pair or real. In the case of three real roots, there are three different possibilities: a triple root,

two roots such that one of them is double, or three different roots. The bistable behavior occurs when three equilibria that correspond to the three different real roots of Eq. (24) exist. To determine the ranges of the parameters ensuring the existence of three real roots, the parameter values at which the complex roots turn to the real ones could be identified. These turning points in the parameter space can be found by obtaining the conditions for the presence of repeated roots.
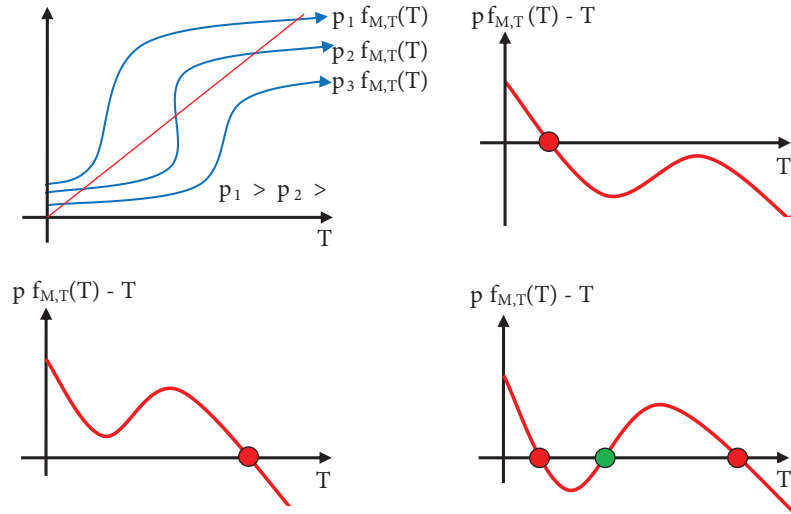
Figure 2. Geometric analysis of the equilibria.

As also exploited in the literature for different lac operon models [3–5,7–9,11,13], the conditions for a triple root of the polynomial equation in Eq. (24) can be derived by considering the fact that the polynomial itself and its first and second derivatives simultaneously vanish at a triple root:

$$K_1 T^3 - p K_1 T^2 + K T - p = 0, \tag{25}$$

$$3 K_1 T^2 - 2 p K_1 T + K = 0, \tag{26}$$

$$6 K_1 T - 2 p K_1 = 0. \tag{27}$$

The above equations show that a triple root appears at $T = p/3$ when $K = 9$ and $K_1 = 27/p^2$. It is interesting to note that $K > 9$ is derived in the literature [3,8] as the bistability condition for different lac operon models. By this derivation, one can conclude that $K = 9$ is a boundary of the bistability interval for K only when the parameters K_1 and p satisfy $K_1 = 27/p^2$. As will be seen in the discriminant, a bistability condition other than $K > 9$ becomes valid when $K_1 > 27/p^2$. For these cases, the boundary for the bistability region is derived by considering the two real roots such that one of them is double. This derivation will be performed in Section 4 by calculating the discriminant of the polynomial in Eq. (24).

3.3. Local stability analysis

Local stability analysis of the state model in Eqs. (1)–(3) for constant G_e and T_e inputs can be realized by determining the location of the eigenvalues of the Jacobian matrix in the framework of Lyapunov's first method

[12]. For the sake of simplicity, one can transform Eqs. (1)–(3) into the following form:

$$\frac{1}{\gamma_M}\frac{dM}{dt} = \frac{\alpha_M}{\gamma_M}f_{M,T}(T)\,f_{M,Ge}(Ge) - M \tag{28}$$

$$\frac{1}{\gamma_P}\frac{dP}{dt} = \frac{\alpha_P}{\gamma_P}M - P, \tag{29}$$

$$\frac{1}{\gamma_T}\frac{dT}{dt} = \frac{\alpha_T}{\gamma_T}f_{T,Te}(Te)\,f_{T,Ge}(Ge)\,P - T. \tag{30}$$

By this transformation, the locations of the eigenvalues of the Jacobian matrix remain in the same half-plane of the complex plane. This fact can be seen from Eq. (31), showing that the eigenvalues λ of the Jacobian matrix related to the transformed model in Eqs. (28)–(30) are just the scaled versions of the eigenvalues $\hat{\lambda}$ for the original model of Eqs. (1)–(3), namely $\lambda = \frac{\hat{\lambda}}{\gamma_i}$ with $\gamma_i > 0$.

$$det\left(\hat{\lambda}I - \hat{J}\right) = det\left(\hat{\lambda}I - diag(\gamma_M, \gamma_P, \gamma_T)J\right) = \gamma_M\gamma_P\gamma_T det\left(\lambda I - J\right) = 0 \tag{31}$$

Here, $\hat{J}$ and J are the Jacobian matrix at a certain equilibrium point T^* for the original and the transformed model, respectively. The eigenvalues of the transformed model are determined by finding the roots of the characteristic equation given in Eq. (32).

$$
\begin{aligned}
det\left(\lambda I - J\right) &= \begin{vmatrix} \lambda+1 & 0 & -\frac{\alpha_M}{\gamma_M}f_{M,G_e}(G_e)\frac{d}{dT}f_{M,T}(T^*) \\ -\frac{\alpha_P}{\gamma_P} & \lambda+1 & 0 \\ 0 & -\frac{\alpha_T}{\gamma_T}f_{T,T_e}(T_e)\,f_{T,G_e}(G_e) & \lambda+1 \end{vmatrix} \\
&= \lambda^3 + 3\lambda^2 + 3\lambda + 1 - p\frac{d}{dT}f_{M,T}(T^*)
\end{aligned}
\tag{32}
$$

To apply the Routh–Hurwitz test for deciding if there exists any eigenvalue in the right-half plane for the equilibrium point T^*, the Routh array is constructed in the Table. Since $f_{M,T}(T)$ is monotonically increasing, then the third term in the first column is always strictly positive. Therefore, the sign change in the first column can occur only when $p\frac{d}{dT}f_{M,T}(T^*) > 1$. It can be seen from the equilibrium equation $pf_{M,T}(T) - T = 0$ together with the positiveness of the initial value $1/K$ of the monotonically increasing function $f_{M,T}(T)$ that, for the case of the three different equilibria, the smallest and the largest equilibrium points both arise when $p\frac{d}{dT}f_{M,T}(T^*) < 1$ and the middle equilibrium point arises when $p\frac{d}{dT}f_{M,T}(T^*) > 1$. Thus, the middle equilibrium point is seen to be unstable while the other two are stable. It can be concluded that the parameter region ensuring the existence of three different equilibria is indeed the bistability region of the lac operon model in Eqs. (1)–(3). This bistability region in the $p - K - K_1$ parameter space will be characterized by discriminant-based bistability analysis method in Section 4.

Table. Routh array for the characteristic equation of the transformed model.

λ^3	1	3
λ^2	3	$1 - p\frac{d}{dT}f_{M,T}(T)$
λ^1	$\frac{1}{3}\left(8 + p\frac{d}{dT}f_{M,T}(T)\right)$	
λ^0	$1 - p\frac{d}{dT}f_{M,T}(T)$	

4. Discriminant-based bistability analysis of the lac operon model

The discriminant Δ of Eq. (24) is given by:

$$\Delta = -4K_1^3 p^4 + \left(18K_1^2 K - 27K_1^2 + K_1^2 K^2\right) p^2 - 4K_1 K^3. \tag{33}$$

Since the discriminant of a polynomial is proportional to the product of the squares of pairwise differences between its roots, Δ becomes zero when a double or a triple root exists. Positive values of Δ correspond to the case of three different real roots of the equilibrium equation in Eq. (24). To obtain the conditions on the parameters, the discriminant equation, i.e .$\Delta = 0$, can be solved in terms of one of the parameters while holding the others fixed. In order to determine the range of p, one can find the p values satisfying $\Delta = 0$ as follows:

$$p^{(1,2)} = \sqrt{\frac{a \pm \sqrt{b}}{8K_1}}, \tag{34}$$

$$p^{(3,4)} = -\sqrt{\frac{a \pm \sqrt{b}}{8K_1}}, \tag{35}$$

where,

$$a = K^2 + 18K - 27, \tag{36}$$

$$b = K^4 - 28K^3 + 270K^2 - 972K + 729. \tag{37}$$

To identify the interval of p where $\Delta > 0$, one can first find the real p roots of $\Delta = 0$. When the inequality in Eq. (38) is not satisfied, $\Delta = 0$ has 4 complex roots, and hence there is no any p value yielding $\Delta > 0$ since $-4K^3$, which is the greatest power of p in Eq. (33), is always negative due to the positiveness of the biological parameter K_1.

$$K^4 - 28K^3 + 270K^2 - 972K + 729 = (K - 1)(K - 9)^3 \geq 0 \tag{38}$$

Therefore, it can be concluded that K values with $1 < K < 9$ do not provide the bistability. One can observe the following relation.

$$a^2 - b^2 = \left(K^2 + 18K - 27\right)^2 - \left(K^4 - 28K^3 + 270K^2 - 972K + 729\right)^2 = 64K^3 > 0 \tag{39}$$

The relation in Eq. (39) implies that a is, in magnitude, greater than $\sqrt{b}$ Then $a > 0$ becomes a necessary condition for the bistability since its violation leads all of $p^{(i)}$'s roots in Eqs. (34) and (35) to be complex, and so there is no p value yielding $\Delta > 0$. Observing $a < 0$ for K values with $0 < K < 1$, all $p^{(i)}$ values in Eqs. (34) and (35) become real only when $K > 9$. In the case of real$p^{(1)}$, $p^{(2)}$, $p^{(3)}$, and $p^{(4)}$, $\Delta > 0$ is obtained for the p values lying in the intervals of $\left(p^{(1)}, p^{(2)}\right)$ and $\left(p^{(3)}, p^{(4)}\right)$, where the latter interval is not valid due to the positiveness of the biological parameter$p$. Hence, the above analysis considering the discriminant $\Delta(p, K, K_1)$ as a function of p provides $p^{(1)} < p < p^{(2)}$, $K > 9$, and $K_1 > 0$ constraints as necessary conditions defining the following region R_{bi}^p.

$$R_{bi}^p = \left\{(p, K, K_1) \in R^3 \,\middle|\, p^{(1)} < p < p^{(2)}, K > 9, K_1 > 0\right\} \tag{40}$$

The whole set of bistability conditions is obtained in the sequel by repeating the above derivations now considering the dependence of $\Delta(p, K, K_1)$ on K_1 and K. The roots of $\Delta(p, K, K_1) = 0$ in terms of K_1, which are obtained as $K_1^{(1)} = 0$ and $K_1^{(2,3)} = \frac{a \pm \sqrt{b}}{8p^2}$, define the region $R_{bi}^{K_1}$ where $K > 9$ and $p > 0$ are required for having real $K_1^{(2,3)}$ roots.

$$R_{bi}^{K_1} = \left\{ (p, K, K_1) \in R^3 \,\middle|\, K_1^{(2)} < K_1 < K_1^{(3)}, K > 9, p > 0 \right\} \tag{41}$$

Similarly, the roots of $\Delta(p, K, K_1) = 0$ by taking K as the variable are obtained as:

$$K^{(1)} = \frac{Kp^2}{12} + \frac{c}{12d} + \frac{1}{12}d, \tag{42}$$
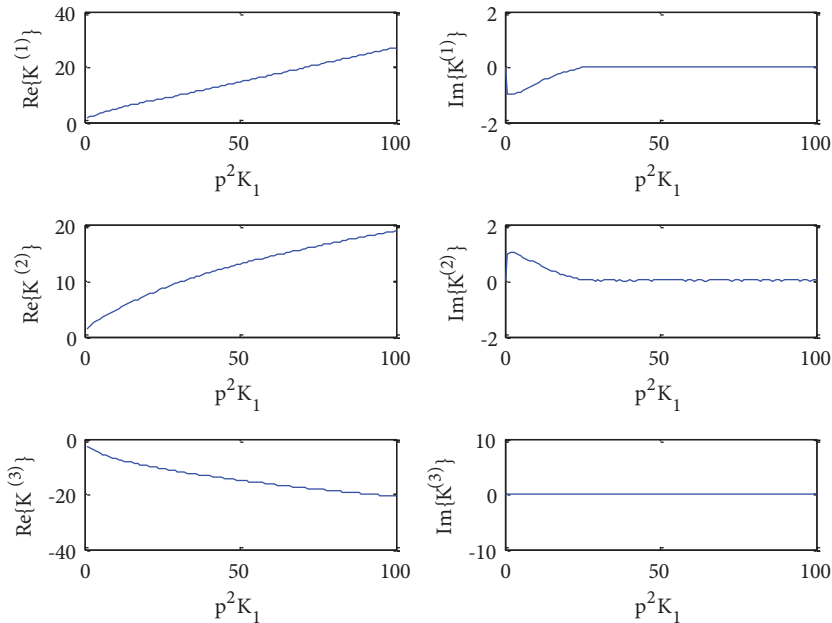
$$K^{(2,3)} = \frac{1}{24} \left(2K_1 p^2 - \frac{\left(1 \mp i\sqrt{3}\right)c}{d} - \left(1 \mp i\sqrt{3}\right)d \right), \tag{43}$$

where c and d are given below.

$$c = K_1 p^2 \left(216 + K_1 p^2\right) \tag{44}$$

$$d = \left(5832 K_1 p^2 - 540 \left(K_1 p^2\right)^2 + \left(K_1 p^2\right)^3 + 24\sqrt{3}\sqrt{-\left(-27 + K_1 p^2\right)^3 \left(K_1 p^2\right)^2} \right)^{\frac{1}{3}} \tag{45}$$

Note that $K^{(1)}$, $K^{(2)}$, and $K^{(3)}$ are functions of $K_1 p^2$ and their highly nonlinear dependency on $K_1 p^2$ can be visualized as in Figure 3.

Figure 3. The $K^{(1,2,3)}$ values for different $p^2 K_1$

The region R_{bi}^K is then defined with the positive and real roots $K^{(1)}$ and $K^{(3)}$ under the condition of $K_1 p^2 > 27$ since K^2 is always a negative real number independent from K_1 and p.

$$R_{bi}^K = \left\{ (p, K, K_1) \in R^3 \,\middle|\, K^{(1)} < K < K^{(3)}, K_1 p^2 > 27 \right\} \tag{46}$$

The above discriminant-based analysis is concluded by defining the bistability region R_{bi} in the $p - K - K_1$ parameter space as the intersection of the derived R_{bi}^p, R_{bi}^K, and $R_{bi}^{K_1}$.

$$R_{bi} = \{(p, K, K_1) \in R^3 \mid p^{(1)} < p < p^{(2)}, K^{(1)} < K < K^{(3)}, K_1^{(2)} < K_1 < K_1^{(3)},$$

$$K_1 p^2 > 27, p > 0, K > 9, K_1 > 0\} \tag{47}$$

Note that $K > 9$ is reported in the literature [3,8] as the bistability condition. However, the above analysis shows that not all K values greater than 9 imply the existence of triple equilibria, but for K values larger than 9 there is always a p value in the interval of $(p^{(1)}, p^{(2)})$ ensuring the existence of triple equilibria. Further note that the $(p^{(1)}, p^{(2)})$ interval actually depends on K and K_1 parameters such that small K_1 and large K values result in a large $(p^{(1)}, p^{(2)})$ interval shifted to the right-hand side; on the contrary, large K_1 and small K values result in a small $(p^{(1)}, p^{(2)})$ interval shifted to the left-hand side.

The bistability conditions derived by discriminant-based analyses are obtained for one of the parameters only, i.e. for $q \in \{p, K, K_1\}$. The three-dimensional bistability region in $p - K - K_1$ space can be constructed by calculating the real roots of the characteristic equation in Eq. (24) for different combinations of the model parameters. The entire bistability region is given graphically in Figure 4. The obtained bistability condition for the K parameter from discriminant-based analysis can be observed from Figure 4. The common result of the literature [3,8], $K > 9$, is determined in this paper as a necessary condition, not only a sufficient one. The K parameter has a lower and an upper limit as obtained from the above discriminant-based analysis.
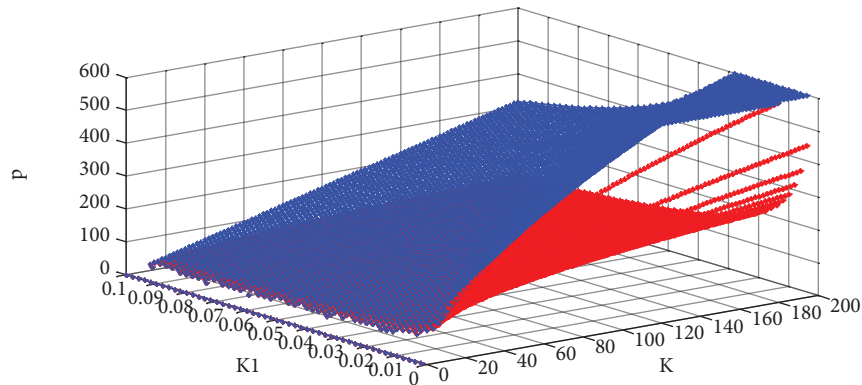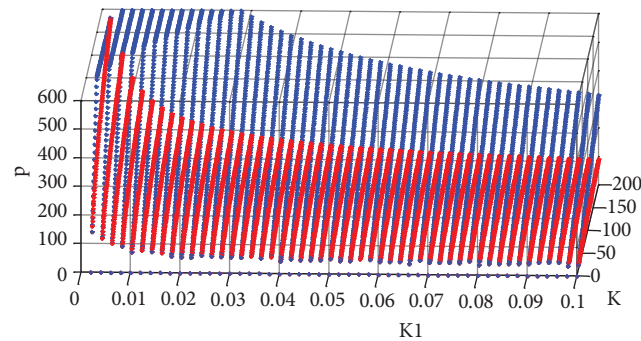

Figure 4. Bistability region in $p - K - K_1$ space.

The two-dimensional intersection of the bistability region R_{bi} with a certain plane defined by keeping K as constant is given in Figure 5. As is observed from Figure 5, the $K_1 p^2 > 27$ condition should also be taken into account to determine the bistability region for the K parameter. When the K_1 parameter value gets larger, the p parameter values that provide a bistability region for the K parameter get smaller.

The 3D and 2D graphical representations of the bistability region depict the bistability region R_{bi} found in Eq. (47).

Figure 5. 2D intersection of bistability region in $p - K - K_1$ space.

5. Conclusion

The bistable behavior of a TMG-induced lac operon model was theoretically investigated in this paper. It was shown that the state variables of the mathematical model, mRNA, permease, and internal TMG, are bounded, and that bistable behavior appears when there exist three equilibria, two of which are stable and one of which is unstable. The main contribution of the paper is the determination of the entire ranges of the model parameters ensuring the bistable behavior of the considered TMG-induced lac operon model by using a discriminant-based analysis.

The proposed discriminant-based method, which defines a parametric equilibrium analysis of the lac operon model, provides a solution to the problem of analysis of the lac operon and other gene regulatory network models under parameter uncertainties. The determined bistability ranges may give an explanation of the variations in the appearance of the bistable behavior of the E. coli lac operon observed in experimental studies. The bistability ranges may also lead to derive new efficient feedback and/or optimal control methods for the regulation of the behavior of the lac operon while optimizing some performance measures.

Acknowledgments

References

[1] Jacob F, Perrin D, Sanchez C, Monod J. L'operon: groupe de gene a expression par un operatour. C R Acad Sci 1960; 250: 1727–1729 (in French).

[2] Novick A, Wiener M. Enzyme induction as an all-or-none phenomenon. P Natl Acad Sci USA 1957; 43: 553–566.

[3] Özbudak M, Thattai M, Lim HN, Shraiman BI, Van Oudenaarden A. Multistability in the lactose utilization network of *Escherichia coli*. Nature 2004; 42: 737–740.

[4] Yıldırım N, Santillan M, Horike D, Mackey MC. Dynamics and bistability in a reduced model of the lac operon. Chaos 2004; 4: 279–292.

[5] Danchin A. Cells need safety valves. BioEssays 2009; 31: 769–773.

[6] Wong P, Gladney S, Keasling JD. Mathematical model of the lac operon: inducer exclusion, catabolite repression, and diauxic growth on glucose and lactose. Biotechnol Prog 1997; 13: 132–143.

[7] Avcu N. Analysis of bistability behaviour of lac operon by using systems theory. PhD, Dokuz Eylül University, İzmir, Turkey, 2013.

[8] Van Hoek MJ, Hogeweg P. In silico evolved lac operons exhibit bistability for artificial inducers, but not for lactose. Biophys J 2006; 91: 2833–2843.

[9] Julius A, Halasz A, Sakar S, Harvey R, Pappas GJ. Stochastic modeling and control of biological systems: the lactose regulation system of *E. coli*. IEEE T Automat Contr 2008; 53: 51–65.

[10] Yagil G, Yagil E. On the relation between effector concentration and the rate of induced enzyme synthesis. Biophys J 1971; 11: 11–27.

[11] Santillan M, Mackey MC. Influence of catabolite repression and inducer exclusion on the bistable behavior of the lac operon. Biophys J 2004; 86: 1282–1292.

[12] Vidyasagar M. Nonlinear System Analysis. Upper Saddle River, NJ, USA: Prentice Hall, 1972.

[13] Avcu N, Demir GK, Pekergin F, Alyürük H, Çavaş L, Güzeliş C. Boundedness and local stability analysis for a TMG induced lac operon model. In: ELECO2012 Elektrik-Elektronik ve Bilgisayar Mühendisliği Sempozyumu; 29 November–1 December 2012; Bursa, Turkey. pp. 420–425 (in Turkish with abstract in English).